Article

# Oxygen Electroreduction through a Superoxide Intermediate on Bi-Modified Au Surfaces

Xiao Li, and Andrew A. Gewirth

*J. Am. Chem. Soc.*, **2005**, 127 (14), 5252-5260• DOI: 10.1021/ja043170a • Publication Date (Web): 16 March 2005



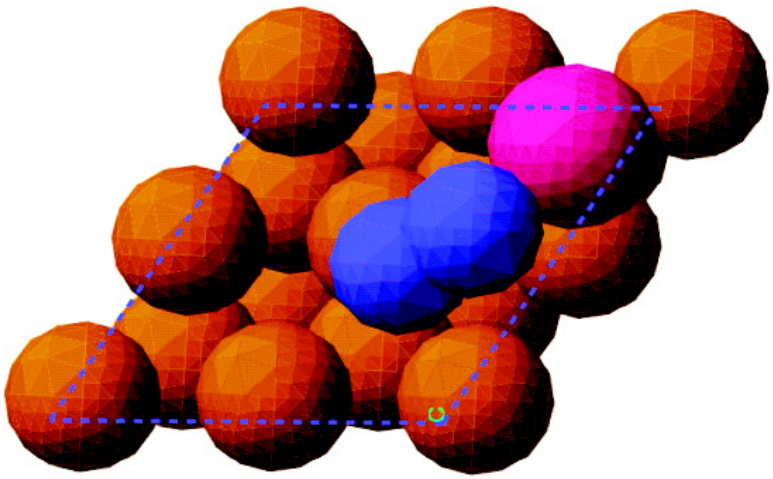

## More About This Article

Additional resources and features associated with this article are available within the HTML version:

- Supporting Information
- Links to the 4 articles that cite this article, as of the time of this article download
- Access to high resolution figures
- Links to articles and content related to this article
- Copyright permission to reproduce figures and/or text from this article

View the Full Text HTML

J|A|C|S
ARTICLES
Published on Web 03/16/2005

# Oxygen Electroreduction through a Superoxide Intermediate on Bi-Modified Au Surfaces

Xiao Li and Andrew A. Gewirth*

*Contribution from the Department of Chemistry, 600 South Mathews Avenue, University of Illinois at Urbana−Champaign, Urbana, Illinois 61801*

Received November 12, 2004; E-mail: agewirth@uiuc.edu

***Abstract:*** The mechanism of the electroreduction of oxygen on bare and Bi-submonolayer-modified Au(111) surfaces is examined using surface enhanced Raman scattering (SERS) measurements along with detailed density functional theory (DFT) calculations. The spectroscopy reveals the presence of superoxide-level species at potentials where oxygen is reduced. These species are not present in solutions absent either oxygen or Bi at these potentials. The spectroscopy also reveals the presence of Bi−OH species which are associated with peroxide reduction. Detailed calculations show oxygen associates much more strongly with Bi in the ($2 \times 2$) configuration on Au(111) relative to the bare Au surface. Additionally, the O−O bond is elongated following $O_2$ association, which follows as a consequence of Bi−O bond formation and partial oxidation of the Bi adatom. These results show for the first time that the four-electron electroreduction of oxygen electroreduction occurs via a series pathway on the Bi-modified surface in acid solution.

## I. Introduction

Because of its important role in corrosion and fuel cells, oxygen electroreduction has long been the focus of electrochemical research.[1] In the acid media most relevant to fuel cells, oxygen electroreduction proceeds by two pathways depending on electrode composition: a direct four-electron pathway, as shown in eq 1

$$O_2 + 4H^+ + 4e^- \rightarrow 2H_2O \quad E^0 = 1.229 \text{ V vs NHE} \quad (1)$$

or a peroxide intermediate-based two-electron pathway, as shown in eqs 2 and 3.

$$O_2 + 2H^+ + 2e^- \rightarrow H_2O_2 \quad E^0 = 0.67 \text{ V} \quad (2)$$

$$H_2O_2 + 2H^+ + 2e^- \rightarrow 2H_2O \quad E^0 = 1.77 \text{ V} \quad (3)$$

For example, on Pt and Ag surfaces, oxygen reduction proceeds by the four-electron pathway, whereas on Au surfaces, the two-electron process dominates and peroxide is produced.[1,2] The high dissociation energy of $O_2$, 494 kJ/mol, leads to slow kinetics and large overpotentials for the four-electron pathway, even on Pt. Unfortunately, the relatively slow kinetics of the reaction makes necessary imposition of high overpotentials on these surfaces with consequent lower efficiency for the process. Additionally, the cost of Pt materials can be prohibitive. Due to these factors, there is an intensive search for materials to replace Pt. One impediment in this search is a lack of understanding concerning the detailed mechanism of $O_2$ electroreduction on Pt or indeed on any relevant electrode material in the acid electrochemical environment.[2]

Efforts directed at obtaining insight into the mechanism of oxygen electroreduction on metal electrode surfaces have relied extensively on voltammetric methods, especially those involving rotating ring disk electrode (RRDE) voltammetry.[1] On the basis of analysis of ring and disk currents for both polycrystalline[3] and single crystal electrodes,[4,5] several different mechanistic pathways for the four-electron reduction of $O_2$ have been proposed. Specific mechanisms involve the so-called "direct" pathway, the "series" pathway, and assorted combinations of these called the "parallel" or "interactive" pathways. The direct pathway features a four-electron pathway (eq 1) without detection of hydrogen peroxide on the ring, while the series pathway is a sequential two- and/or four-electron reduction (eqs 2 and 3) with the detection of hydrogen peroxide.[6]

Discrimination between the different pathways is usually based on models of the ring and disk response along with the presence or absence of detectable intermediates at the ring. For example, $O_2$ electroreduction on Pt and Pt family cathodes, the most extensively studied case, is suggested to occur in the parallel mechanism, with predominate direct four-electron mechanism.[7] However, there is a realization that modeling the RRDE response cannot definitively determine the mechanism

(1) Adzic, R. In *Electrocatalysis*; Lipkowski, J., Ross, P. N., Eds.; Wiley-VCH: New York, 1998.
(2) Markovic, N. M.; Schmidt, T. J.; Stamenkovic, V.; Ross, P. N. *Fuel Cells* **2001**, *1*, 105−116.
(3) Sayed, S. M.; Juettner, K. *Electrochim. Acta* **1983**, *28*, 1635−1641.
(4) Markovic, N.; Gasteiger, H.; Ross, P. N. *J. Electrochem. Soc.* **1997**, *144*, 1591−1597.
(5) Anastasijevic, N. A.; Vesovic, V.; Adzic, R. R. *J. Electroanal. Chem. Interfacial Electrochem.* **1987**, *229*, 305−316.
(6) Anastasijevic, N. A.; Vesovic, V.; Adzic, R. R. *J. Electroanal. Chem. Interfacial Electrochem.* **1987**, *229*, 317−325.
(7) O'Grady, W. E.; Taylor, E. J.; Srinivasan, S. *J. Electroanal. Chem.* **1982**, *132*, 137−150.


**10.1021/ja043170a CCC: $30.25** 

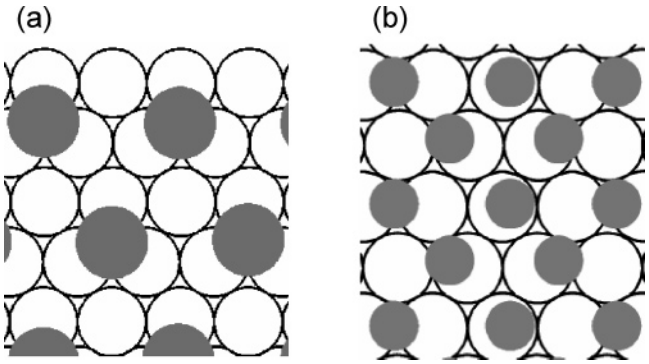


***Figure 1.*** Structures found for Bi upd on Au(111), showing Bi (dark circle) and the Au(111) lattice (open circle) (a) (2 × 2) structure and the (b) ($p \times \sqrt{3}$) structure.

nor can it report on intermediates, possibly strongly held at the disk electrode, not detected at the ring. Spectroscopic data reporting on these intermediates are, to date, lacking. In particular, there is no definitive evidence concerning the existence of a superoxide intermediate in oxygen electroreduction on any surface in acid media. Observation of such an intermediate is important because it would speak to the first stages of the electroreduction event.

An interesting model system for the four-electron reduction of oxygen to water is provided by the underpotential deposition (upd)[8] of Bi on Au(111) surfaces. In acid media, oxygen reduction occurs in a two-electron pathway on bare Au surfaces with $H_2O_2$ as the final product of the reaction.[9] However, modification of the surface with a Bi adlattice catalyzes both oxygen and hydrogen peroxide reduction.[10−14]

On the basis of atomic force microscopy, scanning tunneling microscopy, and X-ray scattering data, we showed that two types of Bi adlattice form before the bulk deposition of Bi: a (2 × 2) structure around 0.4 V with a coverage $\Phi = 25\%$ and a denser ($p \times \sqrt{3}$) adlattice at lower potentials with a coverage $\Phi = 63-65\%$, as shown in Figure 1.[15] The Bi-(2 × 2) adlattice is catalytically active toward the electroreduction of both $O_2$ and $H_2O_2$, while the Bi-($p \times \sqrt{3}$) is inactive for peroxide reduction and only weakly active for two-electron reduction of dioxygen.[16] Interestingly, both Bi adlattices on Au(111) were found to be stable on the surface during the electroreduction process in the presence of oxygen.[17] Further, we showed using a combination of surface enhanced Raman spectroscopy (SERS) and computational means that the origin of the catalytic activity for peroxide reduction on the Bi-(2 × 2) adlattice arose from the adventitious Bi−Bi distance, across which cleavage of the O−O bond to form two Bi−OH moieties could occur. The electron-transfer step involved the reduction of the Bi−OH.[14]

In this paper, we use vibrational spectroscopy to examine intermediates associated with $O_2$ reduction on the Bi-(2 × 2) adlattice. In situ vibrational spectroscopies can provide important information about the interaction of molecules with the immersed electrode surface. Surface infrared spectroscopy is limited by interferences from solution above the electrode surface and its low sensitivity in the low frequency region, below 800 $cm^{-1}$, where metal−oxide and metal−hydroxide modes typically occur.[18] A tantalizing alternative is presented by surface enhanced Raman spectroscopy (SERS), which combines requisite surface sensitivity with the ability to obtain information in the low wavenumber region.[19−23] These advantages have a corresponding cost in issues related to the indeterminacy of enhancement mechanism and the requirement of a roughened surface, which can make detailed comparison between structure and spectroscopy problematic. In this study, SERS on roughened polycrystalline Au is used to study the interaction between upd Bi and $O_2$. Similarities in voltammetry between that from the polycrystalline surface and a well-defined single crystal electrode allow us to make generalizations concerning the relationship between the spectroscopic signals and the electrode surface structure. Correlation of species identified in the spectroscopy with the electrochemical response provides insight into intermediates in the electroreduction reaction, which helps to clarify the mechanism.

## II. Experimental Section

All solutions were prepared from ultrapure water (Milli-Q UVplus, Millipore Inc.; 18.2 MΩ cm). Reagent grade $Bi_2O_3$ (Aldrich, 99.999%), $HClO_4$ (70%, Baker, UltrexII), and $H_2SO_4$ (Baker, UltrexII) were used for preparing solutions. The working electrode for cyclic voltammetric and rotating disk measurement was a polycrystalline Au disk (Monocrystals Inc.) with a diameter of 1 cm. The crystal was annealed for 3 min in a hydrogen flame and quenched by ultrapure water before experiments.

Cyclic voltammograms were obtained in a glass electrochemical cell using an AFRDE5 (Pine Instrument Co.) potentiostat. The counter electrode was a gold wire (Alfa, 99.9985%, 0.5 mm in diameter), which was flame annealed every time prior to use. The reference electrode was a Ag/AgCl cell maintained in a separate compartment connected to the electrochemical cell via a capillary salt bridge to minimize contamination from the reference electrode. All potentials are reported with respect to NHE in this paper. The solutions were deoxygenated by $N_2$ for 1 h and then maintained under $N_2$ or exposed to $O_2$ as appropriate. Rotating disk electrode data were obtained using a Pine Model MSRX rotator equipped with a collet to hold the gold crystal.

The polycrystalline Au was roughened for SERS, and room temperature SERS were obtained as described previously.[14]

Calculations on periodic structures were carried out using CASTEP[24] in MSI-Cerius2. Density functional theory calculations with the generalized gradient approximation (GGA-PW91) were performed.[25] Ultrasoft pseudopotentials were used to describe the electron−core interactions of Au, Bi, O, and H. Valence states include the 5d and 6s shells for Au, 6s and 6p for Bi, 2s and 2p for O, and 1s for H. The

(8) Kolb, D. M. In *Advances in Electrochemistry and Electrochemical Engineering*; Gerischer, H., Tobias, C. W., Eds.; Wiley: New York, 1978; Vol. 11.
(9) Strbac, S.; Adzic, R. *J. Serb. Chem. Soc.* **1992**, *57*, 835−848.
(10) Adzic, R.; Tripkovic, A.; Atanasoski, R. *J. Electroanal. Chem.* **1978**, *94*, 231−235.
(11) Adzic, R. R.; Markovic, N. M.; Tripkovic, A. V. *Glasnik Hemijskog Drustva Beograd* **1980**, *45*, 399−409.
(12) Juettner, K. *Electrochim. Acta* **1984**, *29*, 1597−1604.
(13) Hara, M.; Nagahara, Y.; Yoshimoto, S.; Inukai, J.; Itaya, K. *J. Electrochem. Soc.* **2004**, *151*, E92−E96.
(14) Li, X.; Gewirth, A. A. *J. Am. Chem. Soc.* **2003**, *125*, 7086−7099.
(15) Niece, B. K.; Gewirth, A. A. *Langmuir* **1996**, *12*, 4909−4913.
(16) Oh, I.; Biggin, M. E.; Gewirth, A. A. *Langmuir* **2000**, *16*, 1397−1406.
(17) Tamura, K.; Ocko, B. M.; Wang, J. X.; Adzic, R. R. *J. Phys. Chem. B* **2002**, *106*, 3896−3901.
(18) Nichols, R. J. In *Adsorption of Molecules at Metal Electrodes*; Lipkowski, J., Ross, P. N., Eds.; VCH: New York, 1992.
(19) Pettinger, B. In *Adsorption of Molecules at Metal Electrodes*; Ross, P. N., Lipkowski, J., Eds.; VCH: New York, 1992.
(20) Campion, A.; Kambhampati, P. *Chem. Soc. Rev.* **1998**, *27*, 241−250.
(21) Pemberton, J. E. In *Handbook of Surface Imaging and Visualization*; Hubbard, A. T., Ed.; CRC Press: Boca Raton, FL, 1995.
(22) Weaver, M. J. *J. Raman Spectrosc.* **2002**, *33*, 309−317.
(23) Tian, Z. Q.; Ren, B. *Annu. Rev. Phys. Chem.* **2004**, *55*, 197−229.
(24) Engler, C.; Hofmann, A. *Z. Phys. Chem.* **2001**, *215*, 461−482.
(25) Bilic, A.; Reimers, J. R.; Hush, N. S.; Hafner, J. *J. Chem. Phys.* **2002**, *116*, 8981−8987.

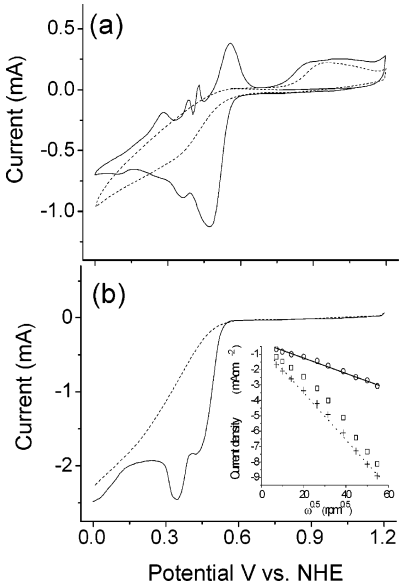


***Figure 2.*** (a) Cyclic voltammogram obtained from Au(poly) in solution containing 0.1 M $HClO_4$ (dotted line) and 0.5 mM $Bi^{3+}$ + 0.1 M $HClO_4$ (solid line), with the scan rate of 25 mV/s. (b) Rotating disk electrode (RDE) voltammogram from Au(poly) in solution containing 0.1 M $HClO_4$ (dotted line) and 0.5 mM $Bi^{3+}$ + 0.1 M $HClO_4$ (solid line), with 400 rpm rotation speed and 25 mV/s scan rate. The inset in (b) shows plots of the current as a function of the square root of the rotation rate. The crosses and open squares represent the maximum current at ca. 0.3 V and the constant current at ca. 0.2 V in solution containing $Bi^{3+}$, respectively. The open circle represents the current at the same potential as that of the cross in solution containing 0.1 M $HClO_4$.

electronic wave functions were expanded in a plane wave basis set with an energy cutoff of 400 eV.[26] For total energy calculations, a Monkhorst−Pack k-point sampling scheme with 12 k-points in the supercell was applied. In this work, the Au(111) surface was modeled by a p(2 × 2) unit cell consisting of three layers and 12 Au atoms. A single Bi adatom on this unit cell mimicked the (2 × 2) structure observed experimentally. As the slab structure was periodic, higher Bi coverages were achieved by adding one or three more Bi atoms to the p(2 × 2) Au slab surface. The vacuum region between slabs was 10 Å. In all cases, surface modifications were applied to only one face of the slab. For Bi adsorption on the Au(111) surface, the topmost gold layer was allowed to relax during the adsorption process, while the other atoms were constrained in their position to mimic the bulk crystal. For $O_2$ adsorption on the Bi/Au(111) surface, only the $O_2$ was allowed to move while the Bi and Au atoms were fixed in place. Calculations for isolated atoms or molecules were performed in the same supercell arrangement as above. Calculations were performed using an SGI Origin 2000 computer at the National Center for Supercomputing Applications (NCSA).

## III. Results and Analysis

**3.1. Electrochemical Behavior. 3.1.1. Cyclic Voltammogram.** Figure 2a shows the cyclic voltammogram for SERS-active Au(poly) in oxygen-saturated 0.1 M $HClO_4$ solution with (solid line) and without (dotted line) 0.5 mM $Bi^{3+}$. In perchloric acid solution not containing Bi, the $O_2$ reduction current begins at ca. 0.5 V (vs NHE) and increases gradually in the cathodic scan. Above 0.9 V, oxidation of Au surface occurs in the anodic scan.

With the addition of $Bi^{3+}$, a large $O_2$ reduction current is observed superimposed on the characteristic Bi upd pattern.[15] Above 0.8 V, surface oxidation is observed on Au. In the cathodic scan around 0.6 V, the onset of $O_2$ reduction coincides with the initial deposition of Bi. The current associated with the sharp reduction peak at 0.47 V is more than 4-fold greater than the cathodic current observed without $Bi^{3+}$. As the potential is scanned more negatively, the reduction current decreases by about a factor of 2 and decreases to a level below that found absent $Bi^{3+}$ at potentials below 0.2 V. The reduction behavior at low potentials is convolved with mass transfer effects and will be clarified by using RDE, described below.

Relative to the voltammetry of $O_2$ reduction obtained from the Bi-modified Au(111) surface,[17] the features observed from Au(poly) in the presence of $O_2$ are broader and match well with the Bi upd peaks on Au(poly).[14] In terms of the potential where the maximum $O_2$ reduction current occurs, our result of 0.47 V agrees well with the 0.49 V found on the Bi-modified Au(111) surface. This suggests that the structural origin of the electroreduction current is associated with the (2 × 2)-Bi adlattice found on parts of the Au(poly) surface.

**3.1.2. RDE Results.** Figure 2b shows the rotating disk electrode voltammogram in the cathodic scan obtained from SERS-active Au(poly) in perchloric acid solution with (solid line) or without (dotted line) $Bi^{3+}$ obtained at a rotation rate of 400 rpm. In perchloric solution, the $O_2$ reduction current begins to flow at ca. 0.5 V and increases gradually as the potential is swept negatively, a behavior observed previously.[9]

In the presence of $Bi^{3+}$, current associated with $O_2$ reduction begins to flow around 0.6 V, and the current is nearly zero at more positive potentials. Around 0.5 V in the cathodic scan, the reduction current rises abruptly and maximizes at around 0.3 V. The maximum current observed in the presence of $Bi^{3+}$ is nearly 3 times that observed in solution containing only perchlorate, indicating the large enhancement of activity due to Bi adlayers on the Au(poly) surface. At more negative potentials, the reduction current decreases as more condensed Bi adlayers form. On the Au(111) surface, this more condensed adlayer is known to be a $\Phi = 0.63-0.65$ ($p \times \sqrt{3}$) structure,[27] while on Au(100), recent STM results show that the more condensed adlattice is associated with $\Phi = 0.65$ ($\sqrt{2} \times 3\sqrt{2}$)-R45° or $\Phi = 0.78$ (4 × 2) structures.[13] Only 78% of the peak current remains at 0.2 V, which indicates the smaller catalytic activity of these more condensed adlattices toward $O_2$ electroreduction. Nevertheless, the current is still larger than that observed in solution without $Bi^{3+}$.

The RDE curve for Bi/Au(poly) reported in Figure 2 matches well with that reported for Bi/Au(111) with regard to both the onset potential and the magnitude of current density with the caveat that determining the current density in the polycrystalline system studied here requires an estimate of the surface roughness. This estimate is achieved through the oxide voltammetry of the polycrystalline surface absent $Bi^{3+}$ and was found to be ca. 2 for the samples used here. This gives a current density at 0.35 V within 25% of that found on the single crystal surface.

The inset in Figure 2b shows the relationship between the $O_2$ reduction current density ($j$) and the square root of the rotation rate ($\omega$) in solutions both with (crosses) and without $Bi^{3+}$ (circles) obtained at the same potentials of 0.3 V, where the maximum current is observed with Bi. The linearity of both curves ($R^2 = 0.991-0.995$; $R$ is the correlation coefficient)

(26) Yourdshahyan, Y.; Zhang, H. K.; Rappe, A. M. *Phys. Rev. B* **2001**, *63*, 1405.

(27) Chen, C. H.; Gewirth, A. A. *J. Am. Chem. Soc.* **1992**, *114*, 5439−5440.

obtained in solution with or without Bi indicates the presence of convection-controlled behaviors, which agrees well with previous studies on single crystalline Au surfaces.[3,9,17]

The $j-\omega^{1/2}$ plot obtained from a solution containing $Bi^{3+}$ at a potential of 0.3 V is indicated by the crosses in the inset. This plot can be analyzed using the Levich equation[28]

$$j_D = 0.62nFD_0^{2/3}\omega^{1/2}\nu^{-1/6}C_0 \quad (4)$$

where $j_D$ is the diffusion-limited current density (mA $cm^{-2}$); $n$ is the number of electrons exchanged in the $O_2$ reduction reaction; $F$ is the Faraday constant; $D_0$ is the diffusion coefficient of $O_2$ ($1.9 \times 10^{-5}$ $cm^{-1}$ $s^{-1}$); $\omega$ is the rotation rate; $\nu$ is the kinematic viscosity ($9.97 \times 10^{-5}$ $cm^2$ $s^{-1}$), and $C_0$ is the bulk concentration of $O_2$ ($1.38 \times 10^{-6}$ mol $cm^{-3}$). Equation 4 can be rewritten as

$$j_D = 0.04n\omega^{1/2} \quad (5)$$

Fitting the data in the inset of Figure 2b yields $n = 3.8$ with an $R^2 = 0.995$. This value of $n$ strongly suggests that $O_2$ electroreduction on Bi-modified Au(poly) at this potential is a four-electron process. Alternatively, the plot obtained from solutions absent $Bi^{3+}$ yields $n = 1.0$ at ca. 0.3 V, which is substantially different from $n = 3.8$ obtained in the presence of Bi.

At lower potential, around 0.2 V, the reduction current remains constant despite the decreasing potential. The open squares in the inset to Figure 1b represent the dependence of the current density on the square root of the rotation rate obtained at 0.2 V. This plot does not fit as well to a linear $j-\omega^{1/2}$ relationship ($R^2 = 0.984$), which implies that the reduction at 0.2 V is controlled by both diffusion and kinetics. For electrode processes with slow kinetics, the Koutecky−Levich equation applies, and the current density can be expressed as

$$j_D = j_K/(1 + j_K/0.04n\omega^{1/2}) \quad (6)$$

where $j_K$ is the kinetic current. Fitting the squares in the inset to eq 3, allowing both $j_K$ and $n$ to vary, results in $j_K = 26$ mA $cm^{-2}$ and $n = 2.8$ ($R^2 = 0.994$) for these lower potentials. Note that if $j_K \gg j_D$, eq 6 is transformed to eq 5. These parameters clearly indicate that the Bi-modified Au surface is much more active at intermediate potentials where the ($2 \times 2$) structure is found on the Au(111) surface than at the lower potentials attendant the formation of the denser adlayer structure.

**3.2. SERS Measurements.** SERS is used to investigate the species on the surface during the $O_2$ electroreduction process. Even though the spectra were recorded at Raman shifts between 300 and 1700 $cm^{-1}$, only the part of the spectra exhibiting features is shown and discussed here. SERS results obtained from SERS-active Au(poly) in deaerated solution ($N_2$ bubbling) containing 0.1 M $HClO_4$ with or without 0.5 mM $Bi^{3+}$ were reported previously.[14]

**3.2.1. SERS with $O_2$ (saturated) + 0.1 M $HClO_4$ on Au-(poly).** Figure 3b shows the SER spectra below 1250 $cm^{-1}$ from Au(poly) in $O_2$ (saturated) solution containing 0.1 M $HClO_4$ at potentials between 0.0 and 1.2 V. For comparison, the SER spectra obtained from the same solution not containing $O_2$ in the same energy region are shown in Figure 3a. In Figure 3a, one peak, labeled peak 1, is observed. Peak 1 at 937 $cm^{-1}$ is well understood to be the symmetric stretch mode of the perchlorate ion, $\nu_s(ClO_4^-)$.[29−31] The intensity of this band is found to increase as the potential is swept to more positive values, consistent with the expected concentration of this anion on or near the electrode surface at potentials above the potential of zero charge (pzc) (ca. 0.5 V).[14]

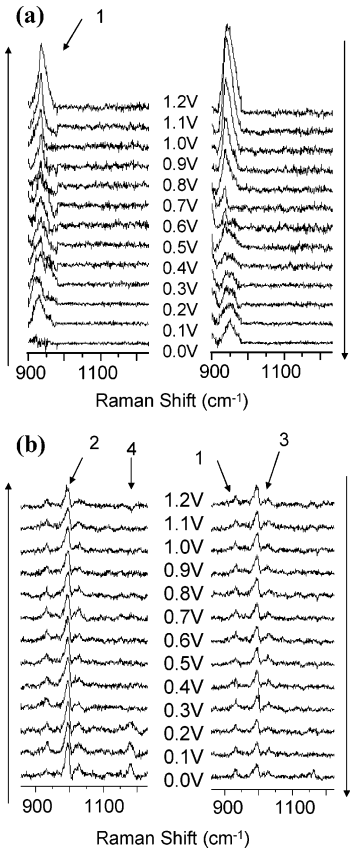


***Figure 3.*** SER spectra between 900 and 1300 $cm^{-1}$ obtained from Au(poly) in solution containing 0.1 M $HClO_4$ (a) saturated with $N_2$ and (b) saturated with $O_2$. The anodic sweep from 0.0 to 1.2 V is shown on the left, and the cathodic sweep is shown on the right.

With $O_2$ in solution, three peaks (labeled 2−4) are observed in addition to peak 1, as shown in Figure 3b. Unlike the case in the deaerated solution, the intensity of peak 1 ($\nu_s(ClO_4^-)$) changes little throughout the entire potential region, which may be due to interference from $O_2$ adsorption or reduction near the surface.

Next, peak 2 at 996 $cm^{-1}$ is assigned to the asymmetric O−H stretch mode of the hydronium ion, $\nu_2(H_3O^+)$.[31,32] Interestingly, even though this peak was not observed in deaerated solution within the potential region studied here (0.0−1.2 V), it was observed at more negative potentials during hydrogen evolution on the Au surface.[33] A peak at this energy was also observed and associated with the adsorption of hydronium at low potential on a Pt(111) electrode surface using infrared spectroscopy.[34]

(28) Bard, A. J.; Faulkner, L. R. *Electrochemical Methods: Fundamentals and Applications*, 2nd ed.; John Wiley & Sons: New York, 2001.
(29) Karelin, A. I.; Grigorovich, Z. I. *Spectrochim. Acta, Part A* **1976**, *32A*, 851−857.
(30) Ratcliffe, C. I.; Irish, D. E. *Water Sci. Rev.* **1986**, *2*, 149−207.
(31) Ratcliffe, C. I.; Irish, D. E. *Can. J. Chem.* **1984**, *62*, 1134−1144.
(32) Giguere, P. A.; Guillot, J. G. *J. Phys. Chem.* **1982**, *86*, 3231−3233.
(33) Li, X. Dioxygen Reduction on Electrode Surfaces. Ph.D. Thesis, University of Illinois, 2004.
(34) Hirota, K.; Song, M.-B.; Ito, M. *Chem. Phys. Lett.* **1996**, *250*, 335−341.

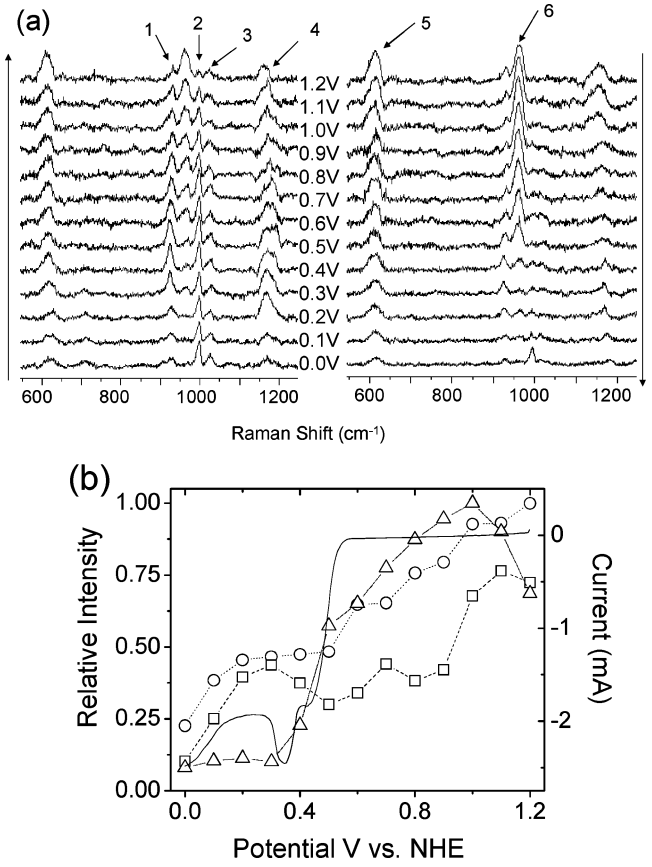


***Figure 4.*** (a) SER spectra obtained from Au(poly) in solution containing 0.5 mM $Bi^{3+}$ and 0.1 M $HClO_4$ saturated with $O_2$. The anodic sweep from 0.0 to 1.2 V is shown on the left, and the cathodic sweep is shown on the right. (b) Potential dependence of SER spectra intensity (△) from peak 6 $\delta_s(Bi(OH)_2)$, (○) from peak 5 $\nu_{as}(Bi_2O_2)$, and (□) from peak 4 $\nu_s(HO_2)$, overlayed with the cathodic sweep of the RDE voltammogram (at 400 rpm and 25 mV/s) obtained in the same solution (solid line).

As hydroxide begins to form on the surface at high potentials, the $\nu(H_3O^+)$ mode becomes much less intense.

Peak 3 at 1030 $cm^{-1}$ is assigned to the symmetric stretch of $ClO_3$, $\nu_s(ClO_3)$, in molecular $HClO_4$.[31] This peak has almost constant intensity within the potential region examined here, similar to the behavior found with peak 1.

Peak 4 observed at 1165 $cm^{-1}$ is assigned to the O−O stretch mode of superoxide, $\nu(HO_2)$.[35] Superoxide was observed on a Ag surface during the $O_2$ adsorption process in the gas phase environment.[36] This band exhibits almost no intensity at positive potentials where no $O_2$ reduction activity is found. However, the intensity of this peak increases at low potentials, starting at ca. 0.0 V and persisting until 0.2 V in the anodic scan. On the cathodic scan, the 1165 $cm^{-1}$ feature reappears when the potential reaches 0.0 V. These are potentials at which two-electron reduction activity of $O_2$ is observed on the bare Au surface. The presence of this mode strongly suggests that superoxide is one of the intermediates for the $O_2$ electroreduction on the bare Au(poly) surface, albeit at the relatively negative potentials attendant this reactivity.

**3.2.2. SERS with $O_2$ (saturated) + $Bi^{3+}$ + 0.1 M $HClO_4$.**

**3.2.2.1. Low Energy Region.** Figure 4 shows the SER spectra from Au(poly) in $O_2$ (saturated) solution containing 0.5 mM $Bi^{3+}$ + 0.1 M $HClO_4$. Six peaks labeled 1−6 were observed below 1300 $cm^{-1}$. Peak 1, the $\nu_s(ClO_4^-)$ mode, shows nearly constant intensity in the cathodic scan, which is the same as that found without $Bi^{3+}$. The intensity of peak 2, $\nu_2(H_3O^+)$, increases as the potential is swept negatively. This likely results from accumulation of hydronium ion near the surface as $O_2$ electroreduction proceeds. Peak 3, $\nu_s(ClO_3)$, exhibits the same behavior found absent $Bi^{3+}$, as discussed above. Interestingly, peak 4, $\nu(HO_2)$, exhibits a different behavior from that found in solution without Bi and will be discussed later.

With the addition of Bi, two new peaks are observed, peak 5 at 620 $cm^{-1}$ and peak 6 at 964 $cm^{-1}$. Both peaks were observed previously in our study of $H_2O_2$ electroreduction on the Bi-modified Au surface.[14] Peak 5 is assigned to the antisymmetric stretch mode of bismuth oxide tetracycle, $\nu_{as}(Bi_2O_2)$, while peak 6 is attributed to the symmetric bending vibrational mode of bismuth dihydroxide, $\delta_s(Bi(OH)_2)$.

**Potential Dependence of Peaks 4, 5, and 6.** Figure 4b shows the potential dependence of relative intensity for peaks 4, 5, and 6, overlayed with the RDE voltammogram in the cathodic scan. First, the potential dependence of $\nu(HO_2^-)$ is examined. Indicated by the open squares in Figure 4b, peak 4 has relatively high intensity at positive potentials. The intensity decreases as potential is swept negatively. After a local minimum at around 0.5 V, the intensity of peak 4 maximizes at 0.3 V. Below 0.3 V, the intensity decreases with the negative scan.

The relative intensity of peak 5, $\nu_{as}(Bi_2O_2)$, is high at positive potentials and then decreases until a potential of 0.5 V is reached. Between 0.5 and 0.3 V, the intensity of peak 5 remains flat, indicating the relative stability of this species on the Bi-(2 × 2) adlayer. The intensity drops greatly at more negative potentials where more Bi is deposited on the surface and a denser adlayer forms.

Starting at 1.2 V in the cathodic scan, peak 6, $\delta_s(Bi(OH)_2)$, increases in intensity until a potential of 1.0 V is reached. The presence of AuOH on the surface in this potential region may precipitate BiOH.[14] Below 1.0 V, the intensity of peak 6 decreases as the surface hydroxide is reduced and removed. At around 0.5 V, the intensity of peak 6 drops dramatically and disappears eventually at low potentials. Interestingly, this loss of peak 6 intensity occurs at the potential corresponding to the sharp increase of electroreduction current of $O_2$, as well as the formation of Bi-(2 × 2) adlayer on the Au(111) surface.

**3.2.2.2. High Energy Region.** Figure 5 shows the SER spectra between 1450 and 1700 $cm^{-1}$ obtained from Au(poly) in $O_2$-saturated perchloric acid solution (a) without and (b) with $Bi^{3+}$. In the absence of Bi, only one peak, labeled 7, around 1588 $cm^{-1}$ is observed. Both the intensity and the energy of this peak exhibit little change throughout the potential region studied here, and this peak is also found in the SER spectrum of Au(poly) + 0.1 M $HClO_4$ (deaerated). Additionally, the full width at half max (fwhm) of peak 7 is ca. 100 $cm^{-1}$, which is substantially larger than the fwhm found for vibrational modes in this energy region. For example, the 1612 $cm^{-1}$ water vibrational mode exhibits a fwhm = 60 $cm^{-1}$.[37] Thus, we tentatively assign this broad band as originating from the surface plasmon.

(35) Hunter-Saphir, S. A.; Creighton, J. A. *J. Raman Spectrosc.* **1998**, *29*, 417−419.
(36) McBreen, P. H.; Moskovits, M. *J. Catal.* **1987**, *103*, 188−199.
(37) Chen, Y. X.; Zou, S. Z.; Huang, K. Q.; Tian, Z. Q. *J. Raman Spectrosc.* **1998**, *29*, 749−756.

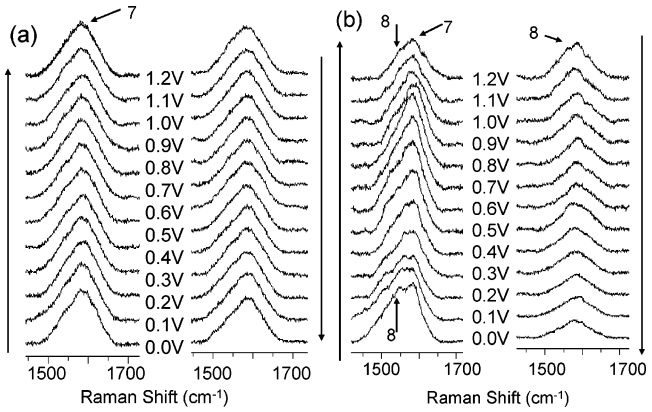


***Figure 5.*** SER spectra between 1450 and 1700 $cm^{-1}$ obtained from Au(poly) in solution containing 0.1 M $HClO_4$ saturated with $O_2$ (a) without and (b) with 0.5 mM $Bi^{3+}$. The anodic sweep from 0.0 to 1.2 V is shown on the left, and the cathodic sweep is shown on the right.

However, in the presence of Bi, Figure 5b shows a new peak (peak 8) at 1550 $cm^{-1}$. The energy of this peak is consistent with that expected for the O−O stretch of $O_2$, which is found at 1556 $cm^{-1}$ in the gas phase.[38−40] Interestingly, this peak is observed at low potentials in the anodic scan, even though these potentials are such that active $O_2$ electroreduction is occurring. As the potential is scanned positively into the surface oxidation region, peak 8 disappears. In the cathodic scan, peak 8 is observed only at the most positive limit. Because peak 8 appears as a shoulder on the much more intense peak 7, any quantification of the potential dependence of the relative intensity of this band is problematic.

**3.3. DFT Calculation Results.** To further understand the interaction between dioxygen and Bi-modified Au surface, we performed DFT calculations to evaluate the interplay of various species on the Au surface during electrocatalysis. Since the Bi-(2 × 2) adlattice on Au(111) is found to be most catalytically active toward $O_2$ electroreduction, the calculations performed here are focused on this structure.

Detailed calculations for the bare Au(111) surface and the Bi-(2 × 2) adlattice on the Au(111) surface have been reported previously.[14] Our calculated Au(111) surface agrees well with experimental results for lattice spacing and surface energy. The 25% coverage of the Bi-(2 × 2) adlattice is modeled through addition of one Bi adatom to the fcc 3-fold hollow site of a (2 × 2) Au(111) surface. For consistency, calculation of $O_2$ is also performed in the same supercell. The calculated bond length of $O_2$ is 1.23 Å, in agreement with the experimental value of 1.21 Å.[41] The potential of zero charge (pzc) for Au(111) in perchloric acid solution is 0.48 V. The Bi-(2 × 2) adlayer begins to form on Au(111) in the potential region around ca. 0.45 V. This suggests that an uncharged surface is a good approximation of the state of electrode.

**3.3.1. $O_2$ Adsorption on Bare Au Surface.** $O_2$ adsorption on the bare Au(111) surface is first examined. Figure 6 shows the optimized geometry of dioxygen adsorption on bare and Bi-modified Au surfaces. As shown in Figure 6a, $O_2$ is adsorbed on an atop site of the bare Au surface and makes an angle of 28° between $O_2$ and the Au surface.

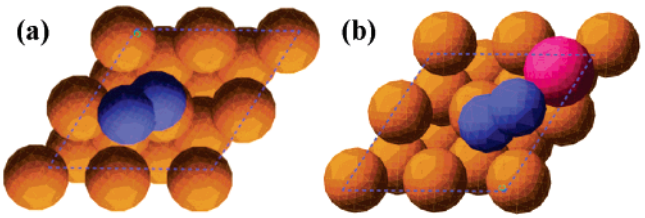


***Figure 6.*** Illustration of the geometry of dioxygen adsorption on the Au-(111) surface. (a) $O_2$ on neutral bare Au and (b) $O_2$ on neutral Bi/Au. Au, Bi, O, and H atoms are orange, pink, blue, and white circles, respectively.

***Table 1.*** Comparison of Dioxygen Adsorption on Bare Au(111) with that on the (2 × 2)-Bi/Au(111) Surface

| | $O_2$/Au | $O_2$/BiAu |
|---|---|---|
| $-E_{ad}$ (eV)[a] | 0.928 | 2.322 |
| $E_{fermi}$ (eV) | −6.567 | −7.342 |
| $\Delta E_{fermi}$ (eV)[b] | 0.175 | 0.677 |
| $q_{Bi}$ (e)[c] | | 1.23 |
| $q_O$ (e) | −0.08 /−0.10 | −0.29 /−0.35 |
| $q_{Au}$ (e) | −0.04 | 0.06 |
| $d_{O-O}$ (Å)[d] | 1.26 | 1.36 |
| $d_{Bi-O}$ (Å)[e] | - | 2.12 |
| $d_{Au-O}$ (Å)[e] | 2.40 | 2.48 |
| $d_{Bi-Au}$ (Å)[e] | - | 2.72 |

[a] The adsorption energy, $E_{ad}$, calculated as the difference between the dioxygen adsorption on the slab energy ($E_{total}$) and the sum of the free dioxygen molecule energy ($E_{O_2}$, $E_{HO_2}$) and the Au or Bi/Au(111) slab energy ($E_{slab}$), with the same external charge. [b] Fermi energy shift due to the adsorption of dioxygen on the surface. [c] Calculated Mulliken charge. [d] O−O bond lengths in free $O_2$, $HO_2$, and $H_2O_2$ are 1.21, 1.28, and 1.46 Å, respectively. [e] Shortest calculated bond length is shown.

Table 1 shows calculated properties for $O_2$ adsorption on bare and Bi-modified Au surfaces. The adsorption energy of $O_2$ on the bare Au surface is −0.928 eV, while the O−O bond of $O_2$ changes little from 1.230 Å of free $O_2$ to 1.26 Å upon adsorption. The shortest distance between O and Au atoms is 2.40 Å, while the calculated Mulliken charge on O is only −0.08 and −0.10 e following exposure to the surface. The Mulliken charges for O in free $O_2$ are, of course, zero. These results suggest that $O_2$ is weakly adsorbed to the bare Au surface.

**3.3.2. $O_2$ Adsorption on the Bi-(2 × 2)/Au Surface.** Figure 6b shows the optimized geometry for $O_2$ adsorbed on the Bi/Au surface. One O atom of $O_2$ is close to the Bi adatom, while the other O is found at an atop site on the Au surface. As Table 1 shows, the adsorption energy of $O_2$ decreases from −0.928 to −2.322 eV following formation of the Bi-(2 × 2) adlattice on the Au(111) surface. This indicates that the Bi adlayer stabilizes $O_2$ adsorption on the Au surface.

Interestingly, the O−O bond of $O_2$ is elongated to 1.36 Å upon adsorption on the Bi/Au surface, which is close to the experimentally found bond length of 1.28 Å for superoxide $O_2^-$.[41] With the adsorption of $O_2$, the calculated Mulliken charge of Bi increases from 0.81 to 1.23 e, while that of the O atoms is calculated to be −0.29 and −0.35 e, respectively. The distance between O and Bi atoms is calculated to be only 2.12 Å, which is within the lengths found experimentally for a Bi−O bond,[42] while the 2.48 Å distance between O and Au atoms is too long for Au−O bond formation.[43] This result strongly suggests that

(38) Valyon, J.; Lonyi, F.; Onyestyak, G.; Papp, J. *Microporous Mesoporous Mater.* **2003**, *61*, 147−158.
(39) Kreutz, J.; Jodl, H. J. *Phys. Rev. B: Condens. Mater.* **2003**, *68*, 214303/1−214303/12.
(40) Berger, A. J.; Wang, Y.; Sammeth, D. M.; Itzkan, I.; Kneipp, K.; Feld, M. S. *Appl. Spectrosc.* **1995**, *49*, 1164−1169.
(41) Nakamoto, K. *Infrared and Raman Spectra of Inorganic and Coordination Compounds*, 3 ed.; Wiley: New York, 1997.
(42) Betsch, R. J.; White, W. B. *Spectrochim. Acta, Part A* **1978**, *34A*, 505−514.
(43) Wang, X.; Andrews, L. *J. Phys. Chem. A* **2001**, *105*, 5812−5822.

the interaction between Bi and O atoms strongly stabilizes the adsorption of $O_2$ on the surface, resulting in elongation of the O−O bond, transfer of electron density to the $O_2$ molecule, and concomitant partial oxidation of the Bi adatom.

## IV. Discussion

The measurements and calculations reported above provide considerable insight to the electroreduction of $O_2$ on Bi-modified Au surface.

**4.1. SERS Measurements.** SERS measurements provide important information concerning the moieties near the surface during the $O_2$ electroreduction process. There are several O-related modes which correspond to the presence of O in different oxidation states at the Au and Bi-modified Au surfaces. Detection of these species by the SERS measurement is confirmation of their participation in the process of $O_2$ electroreduction.

**4.1.1. In $O_2$ (saturated) Perchloric Acid Solution without Bi.** Addition of oxygen to the Au(poly) surface results in the appearance of two new signals relative to the oxygen-free situation. First, the $\nu_2(H_3O^+)$ mode is observed at 996 $cm^{-1}$ in our measurements. The frequency of this mode is highly dependent on environment. For example, $\nu_2(H_3O^+)$ corresponding to a $H_2O\cdots H_3O^+$ structure is found at 1220 $cm^{-1}$, while a frequency of 950 $cm^{-1}$ corresponds to the almost-free hydronium in crystals of large anions, such as $SbClO_6^-$.[32] The relative low energy observed here may be indicative of a small interaction between hydronium and other species in the solution near the Au surface.

Second, perhaps the most important observation obtained from solution not containing Bi is the observation of a band associated with $HO_2$ at low potentials where $O_2$ electroreduction occurs on the Au surface. The observation of this mode provides strong support for the contention that electroreduction of $O_2$ on bare Au proceeds in a stepwise fashion, via a superoxide intermediate.[1,44,45]

Two vibrational bands expected from species that should be present at the interface are absent from spectra obtained from Au(poly) in the presence of $O_2$. First, we observed no signal in the region between 1500 and 1600 $cm^{-1}$ that is attributable to the O−O stretching mode of $O_2$ directly. We note that both our calculations and others[46] show that $O_2$ is very weakly adsorbed to Au(111), and the lack of a substantial interaction may be responsible for the absence of the O−O stretch mode. Second, we were not able to observe a mode associated with $H_2O_2$ (expected around 860 $cm^{-1}$), which should be the result of the second electron transfer event involved in the two-electron reduction of $O_2$ occurring on the bare Au surface.[9] The absence of this mode is possibly associated with the low concentration of peroxide produced and its possibly limited residence time near the surface. We found previously that peroxide is likely only weakly adsorbed on the bare Au surface.[14] Unlike our previous study, which featured a constant peroxide background, the peroxide produced here will diffuse away from the surface readily due to the large concentration gradient.

**4.1.2. In $O_2$ (saturated) $Bi^{3+}$ Solution.** With the addition of $Bi^{3+}$ to the solution, SERS measurements show the presence of several signals attributable to $O_2$, $HO_2$, Bi−OH, and $Bi_2O_2$. The presence of signals associated with all of these species suggests that all play a role during $O_2$ electroreduction.

First, a band at 1550 $cm^{-1}$ is observed, corresponding to the O−O stretch of $O_2$. The frequency of this band is similar to the 1556 $cm^{-1}$ mode of free $O_2$, which suggests that the O−O bond strength is not significantly perturbed upon interaction with the Bi-modified Au surface. Alternatively, the presence of this band, and its absence in solutions lacking Bi, suggests that the $O_2$−surface interaction is more substantial with Bi than without. Indeed, our calculations examining the strength of the $O_2$ interaction on the (2 × 2)-Bi adlattice on Au(111) show that the adsorption energy of $O_2$ on this surface is ca. 1.4 eV less than that found on bare Au(111) alone. This additional stabilization may account for the appearance of the $O_2$ band.

The next O-related band observed in the presence of Bi is that found at 1162 $cm^{-1}$, associated with $HO_2$. (In acid solution, $O_2^-$ occurs as $HO_2$. However, the exact state of the molecule on the Au surface is uncertain from present data.) In solutions absent $Bi^{3+}$, superoxide is detected only at low potentials corresponding to the onset of electroreduction activity. However, in the presence of $Bi^{3+}$, superoxide is detected at all potentials. This band exhibits high intensity at the most positive potentials, declines, or is roughly constant until the onset of electroreduction activity associated with the (2 × 2)-Bi adlattice, and then increases in this potential region before declining again at low potentials. The increase in intensity of $\nu(HO_2)$ between 0.2 and 0.4 V apparently arises as a consequence of the onset of $O_2$ electroreduction activity and suggests that this species is an intermediate in the four-electron electroreduction reaction. The high intensity of the $HO_2$ band at high potentials above 1 V, where the Au surface becomes oxidized, is unexpected. Its presence, and $Bi^{3+}$ and $O_2$ dependence, suggests that some interaction between the oxidized Au surface and these two species must occur. One possibility is that $HO_2$ produced at more negative potentials remains entrained on the surface through some unknown mechanism at these anodic potentials. We did not observe any additional bands at low energy in the SERS that could provide further insight into the nature of this interaction, however. The $HO_2$ band must originate from $O_2$ because our previous work examining $H_2O_2$ electroreduction on the Bi-modified Au surface did not reveal any $HO_2$-associated features which could possibly arise from $H_2O_2$ disproportionation.

Finally, we observe signals at 964 and 620 $cm^{-1}$ associated with Bi−OH and $Bi_2O_2$ species, respectively.[14] These signals were observed previously in our study of $H_2O_2$ reduction on Bi-modified Au and arise due to the spontaneous cleavage of $H_2O_2$ to form these species, with the attendant stabilization due to Bi−O bond formation. We never observed a signal associated with $\nu$(O−O) of $H_2O_2$ directly, in this work, which is consistent with our previous study. As in the case with $H_2O_2$ electroreduction, the intensity of both peaks decreases in the cathodic scan since the Bi−OH moiety formed from peroxide is being reduced. The presence of $\nu_{as}(Bi_2O_2)$ and the similar behavior of $\delta_s(Bi(OH)_2)$ during the hydrogen peroxide and oxygen reduction process strongly suggest that the two reactions have very similar mechanisms on Bi-modified Au surface.

We note that neither peak 5 nor 6 is observed in $O_2$-saturated solution without $Bi^{3+}$. This suggests that the peroxide respon-

(44) Kohler, H.; Goepel, W. *J. Electrochem. Soc.* **1992**, *139*, 3035−3042.
(45) Lu, X.; Faguy, P. W.; Liu, M. *Proc. Electrochem. Soc.* **2003**, *2002−26*, 340−353.
(46) Xu, Y.; Mavrikakis, M. *J. Phys. Chem. B* **2003**, *107*, 9298−9307.

sible for their formation originates from $O_2$, which is decomposed on the Bi-modified Au surface.

**4.2. DFT Calculations.** To clarify the interaction between dioxygen and the electrode surface, we examined the adsorption of $O_2$ on both the bare Au and the Bi-modified Au surfaces by using DFT calculations. Because of the complexity attendant the electron transfer process, only the first stage of the electroreduction (association of $O_2$ with the surface) is modeled here.

$O_2$ is only weakly adsorbed on the Au(111) surface, which agrees well with previous experimental and calculated results.[46,47] With the presence of the Bi-($2 \times 2$) adlayer, the adsorption of $O_2$ is much stronger than that on the bare Au surface, indicated by the $-1.4$ eV lower adsorption energy. The increasing Mulliken charge on Bi and the decreasing charges on O atoms, along with the short Bi−O atom−atom distance, suggest that a bond is formed between Bi and one O atom of $O_2$. Consequently, the calculated O−O bond length of $O_2$ is slightly elongated. Interestingly, the O−O bond is directed toward an adjacent Bi, which is consistent with the participation of this adatom in peroxide reduction, as discussed previously. These calculation results clearly suggest the important role played by the Bi adatom to stabilize $O_2$ on the surface for further electron transfer. Calculations examining the interaction of $HO_2$ with the Bi-modified surface would require a more detailed understanding of the coupled proton−electron transfer to species on the surface and were not attempted here.

**4.3. Mechanistic Considerations.** Those species corresponding to $O_2$, $HO_2$, and the consequences of $H_2O_2$ interaction with Bi (e.g., Bi−OH and $Bi_2O_2$) found in these measurements strongly suggest that all of these species are present during the electroreduction of $O_2$ on Bi-modified Au. The observation that these species are present has immediate consequences for the mechanism of oxygen electroreduction on this surface. In particular, the observation of these species suggests strongly that they are intermediates in the oxygen electroreduction process.

On the basis of both experimental and calculated results, we propose a mechanism for the electroreduction of $O_2$ on the Bi-($2 \times 2$)/Au(111) surface. The initial reactants are free $O_2$ and the ($2 \times 2$)-Bi/Au(111) surface. In the first step, $O_2$ is chemisorbed to one Bi adatom on the surface via the strong interaction between the Bi adatom and one O. After the passage of one electron to $O_2$ through Bi, superoxide forms on the surface. The calculation shows that this electron transfer is likely aided by the elongation of the $O_2$ molecule upon coordination to the Bi adatom. On the basis of a Tafel slope for the four-electron electroreduction of $O_2$ on Pt equal to ca. 120 mV decade$^{-1}$, workers have proposed that the rate-limiting step for $O_2$ electroreduction is the first electron transfer to $O_2$ to make $HO_2$[1] since 120 mV decade$^{-1}$ is the expected slope for a one-electron transfer rate-determining step with a Butler−Volmer transfer coefficient, $\alpha = 0.5$.[28] Unfortunately, the narrow potential window corresponding to the presence of the ($2 \times 2$)-Bi adlattice on Au(111) (visible here as the region of increased electroreduction current between 0.27 and 0.47 V in Figure 2b) makes determination of the Tafel slope for the Bi-catalyzed system problematic. We note that the appearance of a band related to superoxide in the SERS suggests that, at least for some sites on our surface, decomposition of this species is slow enough to allow a signal to be obtained.

When combined with protons from solution, $HO_2$ forms and is chemisorbed on the surface via two Bi adatoms. With a subsequent proton−electron transfer, the peroxide oxidation state level is obtained, and formation of this species leads to the spontaneous cleavage of the O−O bond and formation of two Bi−O bonds. With the addition of an electron and interaction with a proton, $Bi(OH)_2$ is next formed on the surface. Then, the Bi−$(OH)_2$ complex is further reduced with the addition of two more electrons, leading to the cleavage of a Bi−O bond. The Bi center is then formally reduced, and $H_2O$ is formed through interaction with protons in solution.

Four-electron electroreduction of $O_2$ is thought to proceed via two general mechanistic pathways. The first of these, the direct pathway, features the concerted transfer of four electrons to $O_2$. The second, the serial pathway, involves the sequential transfer of four electrons to $O_2$ and to an intermediate species. Combinations of these two limiting cases are also proposed.

Our observation, here, of bands corresponding to $O_2$ and species in various stages of reduction strongly supports involvement of the serial pathway in the mechanism of four-electron $O_2$ reduction on the Bi-modified Au surface. While quantification of the concentration of each of these species is not available from the SERS measurement, their presence, uniquely associated with the four-electron process, does show that each of them must be present during electroreduction activity. This measurement is the first showing directly that some components of the serial mechanism must be operative in $O_2$ electroreduction on the Bi-modified electrode in acid. In particular, it is the first demonstrating the presence of a superoxide intermediate formed during the $4e^-$ reduction of oxygen on any electrode in acid media.

There are several consequences of the establishment of the serial mechanism for four-electron $O_2$ electroreduction. First, this result, coupled with the 120 mV decade$^{-1}$ Tafel slope on Pt, does strongly suggest that renewed attention to the first step, taking $O_2$ to $HO_2$, must be paid. Unclear at this point is whether this step can be enhanced by increasing the interaction of $O_2$ with the surface initially, by changing the nature of the electronic coupling between $O_2$ and the surface, or through other means. Additionally, there is not yet a demonstration that the serial mechanism is operative on more intensively studied materials, such as Pt or Au(100) in basic media.[1]

## 4. Conclusion

$O_2$ electroreduction on a bare Au and Bi-modified Au surface is studied in acid media using both SERS and DFT calculations. While $O_2$ reduction occurs in a two-electron pathway on a bare Au surface and a four-electron pathway on a Bi-modified Au surface, superoxide is observed during the process on both surfaces. This indicates the important role played by superoxide during the $O_2$ electroreduction process on these surfaces. Additionally, the observation of superoxide suggests that the four-electron reduction of $O_2$ on the Bi-modified Au surface occurs in the series mechanism. Furthermore, both SERS measurements and DFT calculations strongly support the formation of Bi−OH during the $O_2$ electroreduction process on the Bi-modified Au surface, which was also observed previously during the $H_2O_2$ electroreduction process on the same surface.

(47) Chesters, M. A.; Somorjai, G. A. *Surf. Sci.* **1975**, *52*, 21−28.

The similarity between the potential-dependent behaviors of the $Bi(OH)_2$ mode observed during both the $O_2$ and $H_2O_2$ electroreduction reactions indicates that the serial mechanism is operative during $O_2$ reduction on this surface.

**Acknowledgment.** X.L. thanks the Department of Chemistry for financial support in the form of a Carl Shipp Marvel fellowship. This work was partially supported by National Computational Science Alliance under CHE030003, and utilized the NCSA Origin2000. The authors thank R. Strange and J. O. White of the Laser Laboratory in the Frederick Seitz Materials Research Laboratory at the University of Illinois for their assistance in Raman data acquisition. The Laser Laboratory is funded by Department of Energy Grant DE-FG02-96ER45439 through the Materials Research Laboratory at the University of Illinois. This work was funded by the NSF (CHE-02-37683), which is gratefully acknowledged.

**Supporting Information Available:** The geometries (Cartesian coordinates) of all calculated slabs are given. This material is available free of charge via the Internet at http://pubs.acs.org.

JA043170A